GEOLOGY | THE GEOLOGICAL SOCIETY OF AMERICA®

https://doi.org/10.1130/G49812.1

Manuscript received 25 October 2021
Revised manuscript received 10 February 2022
Manuscript accepted 20 February 2022

Published online 14 April 2022

Sulfide-associated hydrothermal dolomite and calcite reveal a shallow burial depth for Alpine-type Zn-(Pb) deposits

M. Giorno[1], L. Barale[2], C. Bertok[1]*, M. Frenzel[3], N. Looser[4], M. Guillong[4], S.M. Bernasconi[4] and L. Martire[1]
[1]Department of Earth Sciences, University of Torino, 10125 Turin, Italy
[2]Institute of Geosciences and Earth Resources, CNR-Turin Unit, 10125 Turin, Italy
[3]Helmholtz Zentrum Dresden-Rossendorf, Helmholtz Institute Freiberg for Resource Technology, D-09599 Freiberg, Germany
[4]Department of Earth Sciences, ETH Zürich, CH-8092 Zurich, Switzerland

ABSTRACT

Difficulties in dating Mississippi Valley–type (MVT) mineral deposits and the often closely associated dolomitization have led to controversy regarding their origin. We report the first radiometric ages for the Gorno mining district in northern Italy, an example of the Alpine subclass of MVT deposits. U-Pb ages of hydrothermal carbonates pre- and postdating the ore-forming event show that base-metal mineralization occurred shortly after the deposition of the Carnian host rocks. This implies that the Gorno ore deposits formed at shallow burial depth prior to the Early Jurassic western Tethys rifting phase. Contemporaneous Triassic magmatism and extensional tectonics likely contributed to the high geothermal heat fluxes required to drive the mineralizing system. Our study reinforces the need for reliable geochronological data for metallogenic models and warns against a general application of classic North American MVT models to similar deposits worldwide.

INTRODUCTION

Mississippi Valley–type (MVT) deposits are epigenetic, stratabound, carbonate-hosted sulfide bodies formed by high-salinity, warm fluids (75–200 °C; Leach et al., 2001, 2005). MVT deposits and dolomitization events are often associated. Both are of major economic importance and are genetically related to hydrothermal fluid flow through large rock volumes. Since both the mineralization and the associated dolomitization postdate host-rock deposition, stratigraphy does not constrain the age of hydrothermal activity, except in rare cases, e.g., when mineralized clasts are reworked in intraformational breccias (Schroll et al., 2006; Shelton et al., 2019). Moreover, only few radiometric ages are available for MVT deposits, obtained by Rb-Sr on sphalerite (Ostendorf et al., 2015, 2017), U-Pb/Th-Pb on carbonates (Brannon et al., 1996), and Re-Os on pyrite (Hnatyshin et al., 2015). The difficulties involved in dating host-rock formation, dolomitization, and ore-mineral precipitation have led to contrasting genetic models for MVT deposits. These range from shallow to deep burial conditions and from extensional to compressional tectonic regimes (e.g., Leach et al., 2001; Kesler et al., 2004; Ostendorf et al., 2015).

We present the first radiometric ages for the Alpine-type (APT) deposits of the Gorno mining district in northern Italy. APT deposits are considered to be a subclass of MVT deposits, mostly consisting of stratabound bodies within Anisian–Carnian platform carbonates across the European Alps (Leach et al., 2003). Their genesis is controversial because radiometric ages, only available for the Austrian deposit of Bleiberg, are highly uncertain: Sr and Pb ages of whole rocks yielded uncertainties of ±30 m.y. and ±48 m.y., respectively (Schroll et al., 2006), and Rb-Sr dating on sphalerite provided both Late Triassic and Early Jurassic ages (Henjes-Kunst et al., 2017). Based on the presence of finely laminated ore textures, ore-bearing clasts in sedimentary breccias, and highly negative $\delta^{34}S$ values of the sulfide minerals, some researchers have suggested that several APT deposits formed shortly after, or even during, host-sediment deposition (e.g., Maucher and Schneider, 1967; Brigo et al., 1977; Cerny, 1989; Schroll et al., 2006; Kucha et al., 2010). Other studies have proposed a deep burial setting, based on high fluid-inclusion homogenization temperatures and comparison with classic MVT models (e.g., Jicha, 1951; Omenetto, 1966; Leach et al., 2003; Mondillo et al., 2019).

A precise understanding of the timing and mode of ore formation is not only of scientific interest, but it is also of economic relevance, since it strongly affects current and future exploration. Our U-Pb ages from hydrothermal carbonates associated with the ore minerals, combined with petrographic and fluid inclusion data, provide a major advance in understanding the timing of APT Zn-(Pb) mineralization.

MATERIALS AND METHODS

We investigated 13 carbonate-bearing samples by transmitted light (TL) and cathodoluminescence (CL) microscopy. Fluid inclusion (FI) petrography and microthermometry were carried out on dolomite (doubly polished sections, 110 μm thick). Carbonate U-Pb data were acquired by laser ablation–inductively coupled plasma–mass spectrometry (LA-ICP-MS) on polished thin sections (60 μm) following the methods of Roberts et al. (2017) and Guillong et al. (2020). Details on the samples and analytical procedures are provided in the Supplemental Material[1].

GEOLOGIC SETTING

The Gorno mining district lies in the Southalpine domain (Figs. 1A and 1C), a south-verging retrobelt of the Alpine orogenic wedge, separated from the metamorphosed part of the Alps by the Periadriatic Line. The Southalpine domain consists of a sedimentary succession of Permian to Paleogene age, deformed during the

*E-mail: carlo.bertok@unito.it

[1]Supplemental Material. Extended materials and methods, additional petrographic data for U-Pb geochronology, additional U-Pb data about outlier ages, and additional figures and tables. Please visit https://doi.org/10.1130/GEOL.S.19491488 to access the supplemental material, and contact editing@geosociety.org with any questions.

CITATION: Giorno, M., et al., 2022, Sulfide-associated hydrothermal dolomite and calcite reveal a shallow burial depth for Alpine-type Zn-(Pb) deposits: Geology, v. XX, p. , https://doi.org/10.1130/G49812.1

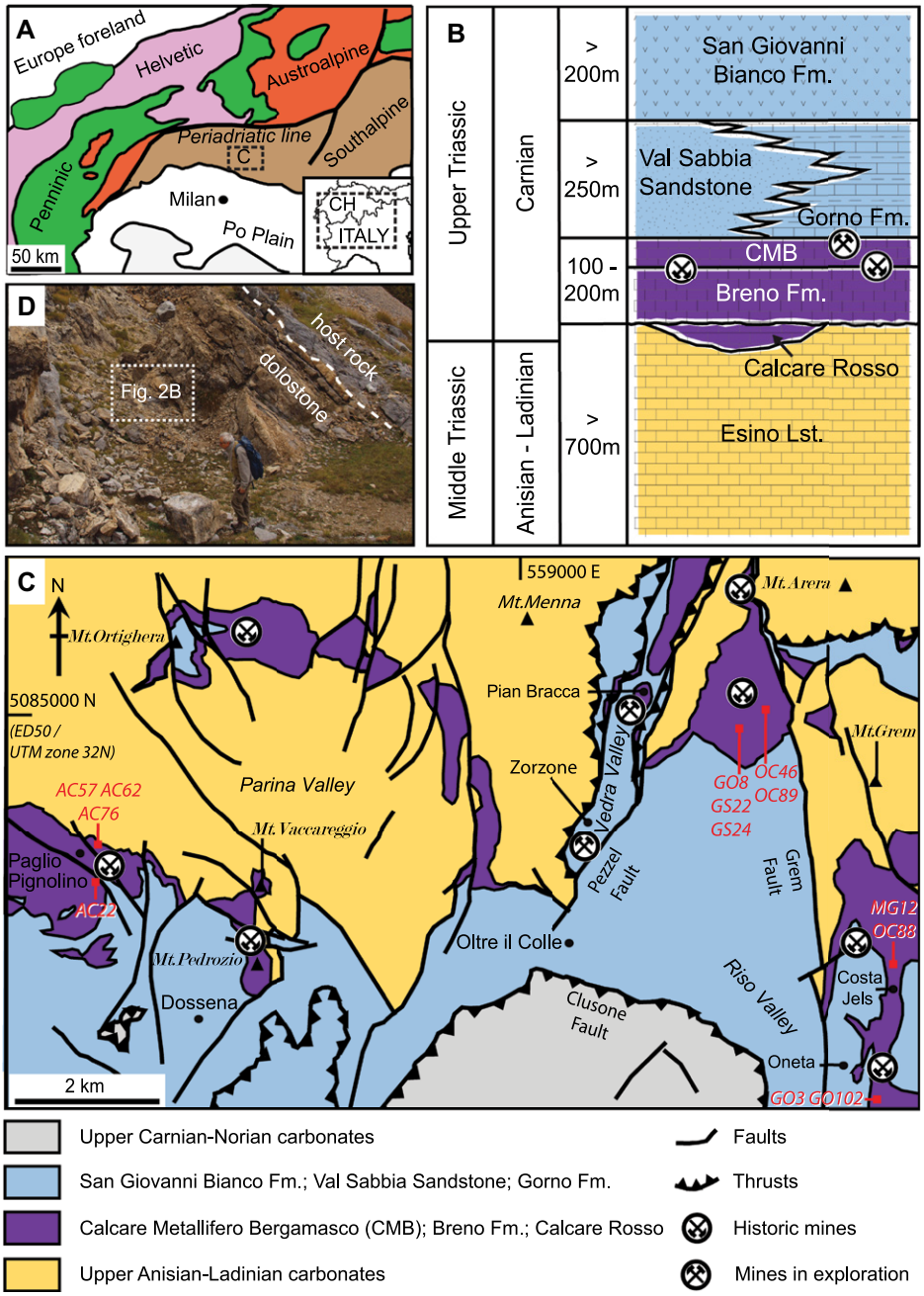

Figure 1. (A) Geologic scheme of the European Alps. CH—Switzerland. (B) Stratigraphic log of the upper Anisian–Carnian succession in the Gorno mining district, showing mineralized horizons. (C) Geologic map of the Gorno mining district showing ore deposits; adapted from Jadoul et al. (2012). (D) Stratabound dolomite Dol-2 body in Calcare Metallifero Bergamasco (CMB) hosting major sulfide mineralization (45°55′15.1″N, 9°48′07.9″E).

Alpine orogeny under nonmetamorphic conditions (Laubscher, 1985; Zanchi et al., 2012; Zanchetta et al., 2015). In the Gorno district, platform carbonate sedimentation took place in the late Anisian (Esino Limestone), ending with emersion of the platform and development of karsts and paleosols (Calcare Rosso; Fig. 1B; Berra and Carminati, 2010; Jadoul et al., 2012). In the early Carnian, deposition of the 50–100-m-thick peritidal limestones of the Breno Formation was followed by the meters- to tens-of-meters-thick peritidal-lagoon facies of the Calcare Metallifero Bergamasco (CMB). A deepening of the basin then led to the deposition of the lagoonal marly limestones of the Gorno Formation (>250 m thick), which laterally pass to the deltaic volcaniclastic sediments of the Val Sabbia Sandstone. In the late Carnian, a return to shallow-water deposition is recorded by the sabkha dolostones and evaporites of the San Giovanni Bianco Formation. The Gorno ore deposits are stratabound and confined to the lower Carnian section (Fig. 1B). They mainly consist of sphalerite, minor galena, fluorite, and barite. High-grade sulfide ore is hosted in the 5–10-m-thick basal unit of the Gorno Formation, consisting of an organic-rich laminated marl and siltstone lithozone, known as "black shales". Other major orebodies are hosted in the peritidal limestones of the Breno Formation and CMB. Mineralization styles include replacements, dissolution cavity fillings, and breccia cements (Omenetto, 1966; Assereto et al., 1977). Deformation of the ore deposits by Alpine faults documents that mineralization occurred at least prior to the Alpine tectonic activity (Mondillo et al., 2019). Current exploration efforts are focused on the Zorzone and Pian Bracca deposits (Fig. 1C) and have identified a total resource of 7.79 Mt at 6.8% Zn, 1.8% Pb, and 32 g/t Ag (Altamin Ltd., 2021).

PARAGENETIC SEQUENCE

A fabric-retentive, early diagenetic dolomite (Dol-1) replaced the micritic matrix of the supratidal laminated sediments of the Breno Formation and CMB. It is fine grained, white in hand specimen, and exhibits bright-red CL. Lags of dolomitized intraclasts at the base of calcareous transgressive subtidal levels show that Dol-1 formed shortly after sedimentation (Fig. 2A). Fenestral pores in both unaltered limestones and Dol-1 dolostones are filled with a sparry calcite cement (Cal-1), commonly nonluminescent or dull-brown and locally zoned under CL (Figs. 3A and 3B).

A complex series of dolomitization, brecciation, dissolution, and cementation phenomena followed Dol-1 and Cal-1 and affected the studied rocks over the entire area (Fig. 4A). Dolomitization gave rise to decametric, tan-colored bodies (replacive Dol-2), either roughly stratiform or, less commonly, discordant to the bedding (Fig. 1D). Replacive Dol-2 forms a mosaic of fine- to coarse-grained euhedral dolomite crystals (30–600 μm; Figs. 2C, 2D, 3C, and 3D). Dol-2 also occurs as coarsely crystalline saddle dolomite cements (up to millimeter size) in pores, veins, burrow infills, and bivalve shells (Figs. 2E, 3C, and 3D). Dol-2 is commonly dull red to almost nonluminescent under CL (Figs. 3D and 3F). Primary FIs in Dol-2 cements yielded homogenization temperatures between ~80 °C and 140 °C (mean value: 111 ± 13 °C; Table S4 in the Supplemental Material). Dol-2 dolostone bodies are locally associated with crackle-to-mosaic breccias with centimeter- to decimeter-sized clasts mainly cemented by sphalerite and a calcite cement younger than Cal-1 (Cal-2, see below; Figs. 2B–2D). A major dissolution phase followed Dol-2 and is documented by irregularly shaped, decimeter- to meter-sized cavities with branches that are either roughly concordant or discordant to bedding (Figs. 2F and 2G). Dissolution cavities show infills of laminated internal sediments consisting of dissolution

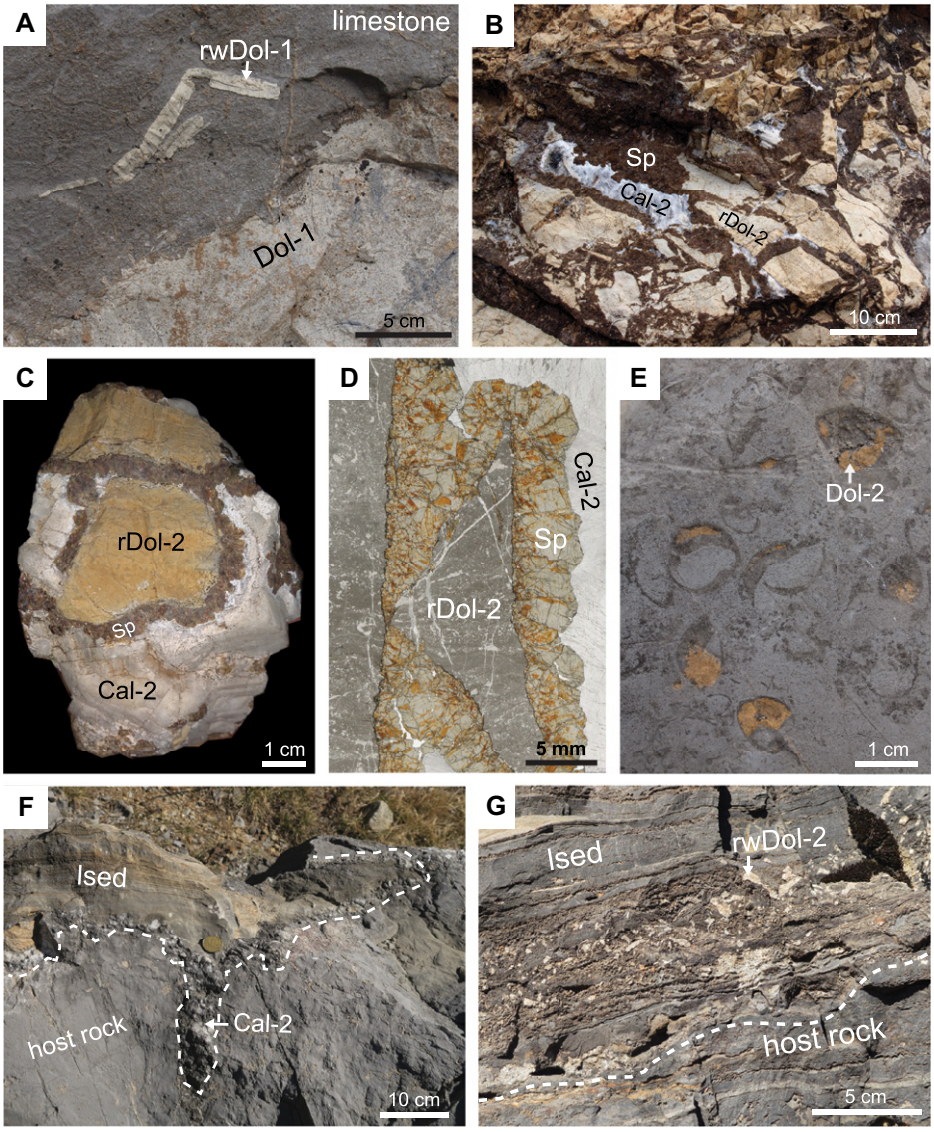

Figure 2. (A) Reworked clasts of early diagenetic dolomite Dol-1 (rwDol-1) at the base of a transgressive subtidal bed in the Calcare Metallifero Bergamasco (CMB) in northern Italy. (B) Stratiform mosaic breccia with clasts of replacive Dol-2 (rDol-2) cemented by sphalerite (Sp) and calcite Cal-2. (C,D) Mesoscopic features (C), and transmitted light photomicrograph of sample OC89 (D), showing rDol-2, sphalerite (Sp), and Cal-2 relationships in mineralized breccias. (E) Bivalve shells in the CMB, partially filled with Dol-2. (F) Dissolution cavity in the Breno Formation (dashed line) infilled by laminated sediments (lsed), resting on euhedral terminations of Cal-2 crystals. (G) Internal sediments in dissolution cavity in the Breno Formation (base delimited by dashed line). Lag of reworked Dol-2 clasts (rwDol-2) passes upward to finer-grained laminated sediments (lsed).

residues such as host-rock clasts and millimeter- to centimeter-sized reworked fragments of Dol-2 cements in a finer carbonate matrix. Internal sediments are cemented by fluorite, Cal-2, or sulfides. A further saddle dolomite generation (Dol-3), mostly dull brown in CL, fills a stockwork of veinlets crossing Dol-2 dolomitized bodies. Locally, Dol-3 syntaxially overgrows Dol-2 cements in larger veins and fenestral pores, and reworked Dol-2 clasts in dissolution cavity infills (Figs. 3C–3F). Homogenization temperatures from primary FIs in Dol-3 cements range between ~80 °C and 140 °C (mean value: 107 ± 12 °C). Euhedral terminations of Dol-3 crystals are overgrown by sphalerite, showing that sulfide precipitation directly followed Dol-3 (Figs. 3C–3F). Sphalerite commonly forms equant crystals up to millimeters in size, occurring both as void-filling cements and as replacement of the carbonate host (Figs. 2B–2D and 3C–3H). A post-sulfide sparry calcite cement (Cal-2), up to centimeters in size, fills the remaining voids in pores, veins, and dissolution cavities (Figs. 2B–2D, and 2F). Cal-2 shows an almost homogeneous bright-yellow CL and, depending on the site, overgrows either Cal-1, Dol-2, Dol-3, or sphalerite (Figs. 3A and 3E–3H). Locally, the Cal-1/Cal-2 boundary is irregular and cuts through CL zones in Cal-1, showing that Cal-2 precipitation occurred after etching of Cal-1 (Fig. 3B); in other places, Cal-2 completely replaced former Cal-1 void-filling cements (e.g., Figs. S6A–S6B). Cal-2 also fills thin veins locally associated in swarms and merging with cavity-filling Cal-2 cements. Commonly, the undolomitized host sediments (Figs. 3A and 3B) show the same bright yellow CL, pointing to large-scale recrystallization coeval with Cal-2. Fluorite may occur together with Cal-2, showing variable geometric relationships, suggesting coprecipitation of the two minerals. In conclusion, only two pore-filling calcite cement generations are recognizable over the whole study area. Therefore, all the yellow-luminescent calcite is referrable to Cal-2 and postdates sphalerite. Additional petrographic data are provided in the Supplemental Material.

CARBONATE U-Pb GEOCHRONOLOGY

In total, nine measurement sites from five carbonate-bearing samples provided robust radiometric ages (Figs. 4B and 4C; Tables S2 and S3; Fig. S2). The earliest dolomite in the paragenetic sequence (Dol-1) yielded an age of 245.8 ± 12.5 Ma (95% confidence interval). Pre-sulfide replacive and void-filling Dol-2 yielded ages of 229.9 ± 11.2 Ma and 227.1 ± 17.9 Ma, respectively, while post-sulfide Cal-2 yielded ages of 232.2 ± 5.2 Ma, 229.0 ± 10.8 Ma, 228.4 ± 5.3 Ma, and 226.9 ± 5.3 Ma. All of these ages fall within a relatively narrow range and overlap or shortly postdate the early Carnian depositional age of the host rocks (ca. 237–232 Ma; Fig. 4B). Two younger ages probably represent resetting at later times rather than younger formation ages (see the Supplemental Material for discussion).

DISCUSSION AND CONCLUSIONS

The U-Pb radiometric ages presented here provide the first robust constraints on the age of ore formation in the Gorno area. The younger age limit is given by the age of 232.2–227.0 Ma of post-sulfide Cal-2, whereas the maximum age is defined by the precipitation of pre-sulfide Dol-2 and by host-rock deposition (early Carnian; ca. 237–232 Ma; Fig. 4B). Therefore, all processes occurring between Dol-2 and Cal-2 precipitation, which include dissolution, brecciation, and sulfide precipitation, must fall in a time window of a few million years after the deposition of the host rocks. Thus, based on the known thicknesses of the overlying sediments (Gorno/Val Sabbia and San Giovanni Bianco Formations, and the lowermost part of Dolomia Principale; Jadoul et al., 2012), we conclude that the burial depth at the time of ore formation was relatively shallow (tens to a few hundreds of meters).

Homogenization temperatures of primary FIs in pre-ore hydrothermal dolomites (Dol-2;

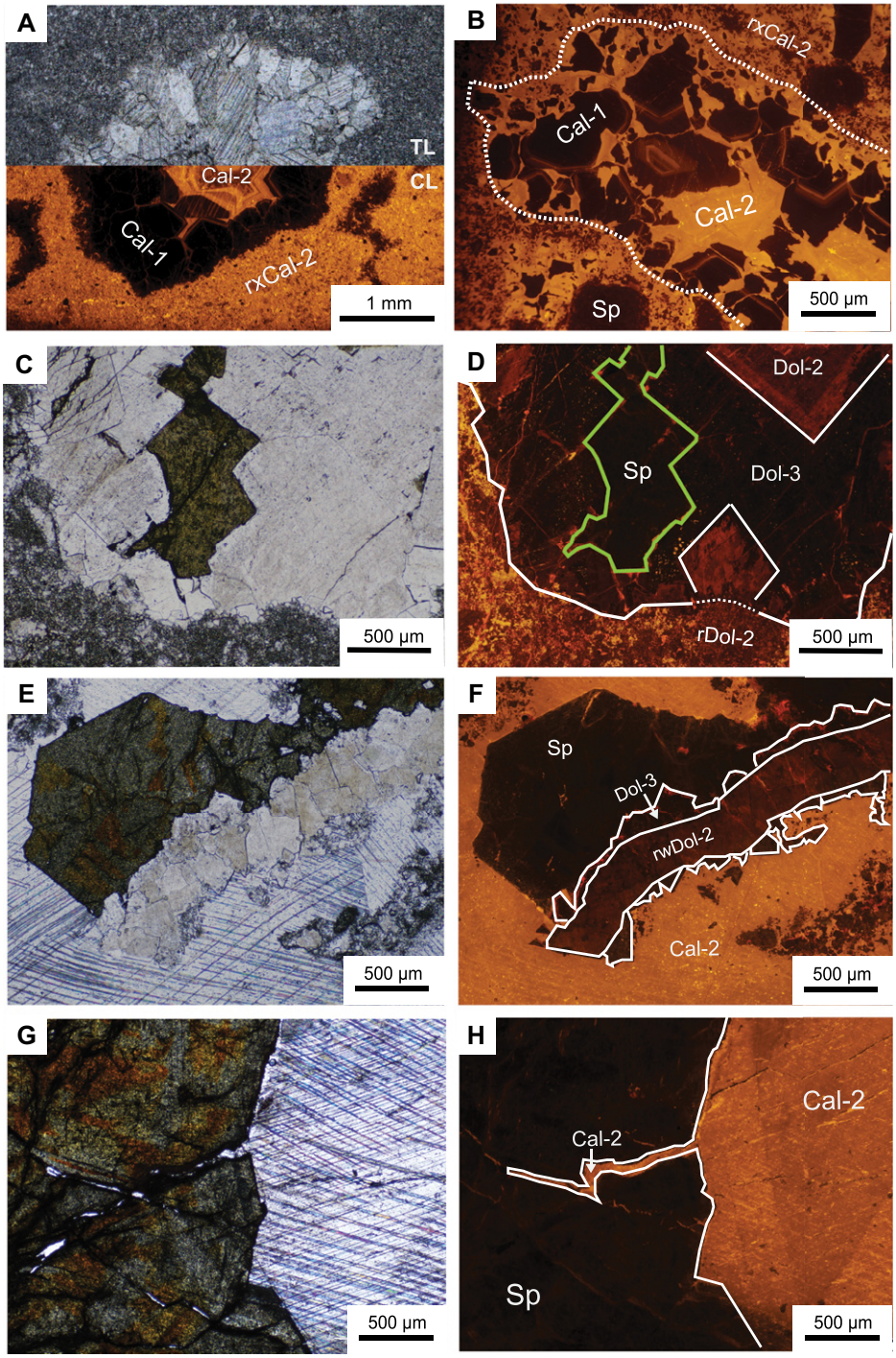

Figure 3. (A,B) Fenestral pores filled with calcites Cal-1 and Cal-2, surrounded by sediment recrystallized by Cal-2 (rxCal2). In B, Cal-1 was affected by dissolution and Cal-2 reprecipitation (A: transmitted light [TL] + cathodoluminescence [CL]; B: CL). (C,D) TL (C) and CL (D) images of a shrinkage pore filled with dolomite Dol-2, Dol-3, and sphalerite (Sp) cements. (E,F) TL (E) and CL (F) images of reworked Dol-2 cements (rwDol-2) in a dissolution cavity, overgrown by Dol-3, sphalerite (Sp), and Cal-2. (G,H) TL (G) and CL (H) images of Cal-2 postdating and filling fractures in sphalerite (Sp).

Dol-3) range between ~80 °C and 140 °C. These results and the observed carbonate paragenesis are closely comparable to those reported for the same area by Hou et al. (2016), who, in the absence of absolute age determinations, interpreted the formation temperatures to be the result of deep burial. However, our new radiometric data and the consequent shallow burial depths show that these temperatures are too high to have been caused by the burial load alone, even assuming a high geothermal gradient of 40 °C/km, which is possible in continental areas of extension (Jaupart and Mareschal, 2007). Thus, our data clearly indicate a thermal disequilibrium between the fluids and host rocks.

High crustal heat flux was likely at that time. In fact, regional magmatism linked to extensional and strike-slip tectonics (Doglioni, 1987; Berra and Carminati, 2010) is well documented in the Southalpine domain during the Anisian–Carnian, related to an early phase of Pangea breakup (De Min et al., 2020, and references therein). In the Gorno district, pyroclastic layers in the lower Carnian Breno Formation and CMB, and volcaniclastic deposits in the overlying Val Sabbia Sandstone provide evidence for magmatism (Jadoul et al., 2012). While a direct genetic link between sulfide mineralization and magmatism cannot be inferred from the available data, it is likely that magmatic activity contributed to the high heat fluxes necessary to drive a hydrothermal system in the Gorno district. Concurrent thermal perturbation and extensional faulting triggered the circulation of fluids, which leached base metals from depth, e.g., from basement rocks, resulting in sulfide deposition within the carbonate sediments.

The classic MVT model, envisaging circulation of basinal brines in foreland settings, was originally defined for the deposits of the Mississippi River basin. This model relates high precipitation temperatures to deep burial, and it has often been applied to other carbonate-hosted Pb-Zn deposits worldwide. However, its general applicability has been challenged, since new geochronologic data showed that MVT deposits can also form at shallow depths in extensional settings, and possibly be related to magmatism (e.g., Twelve Mile Bore and Bloodwood-Kapok in Western Australia—Brannon et al., 1996; Maestrat basin in Spain—Grandia et al., 2000; Irish Midlands—Hnatyshin et al., 2015; Jabali in Yemen—Ostendorf et al., 2015; Tres Marias in Mexico—Ostendorf et al., 2017). The Gorno case represents a further example of an MVT deposit formed at shallow burial depth and in an extensional setting, and it confirms the need for solid geochronological data to construct reliable metallogenic models. In the absence of

Figure 4. (A) Paragenetic sequence showing relative timing of the principal mineral generations. Dashed lines indicate uncertainty ranges. (B) Selected U-Pb ages of carbonate minerals (six measurement sites) with error bars. Red rectangle highlights the overlap interval of calcite Cal-2 ages. (C) Selected Tera-Wasserburg concordia diagrams of ore-related carbonates. Reported uncertainties of lower-intercept age do not include additional 2% relative long-term excess variance (Guillong et al., 2020). See the Supplemental Material (see footnote 1) for full U-Pb age data. Values between vertical bars (x|y|z) are standard error (x) and (95%) confidence interval without (y) and with (z) overdispersion. $(^{207}Pb/^{206}Pb)_0$ is initial lead composition. MSWD—mean square of weighted deviates.

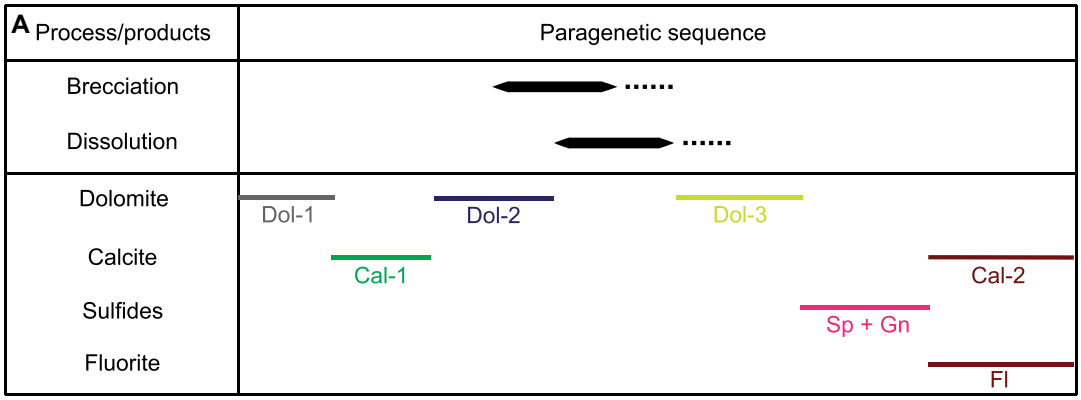

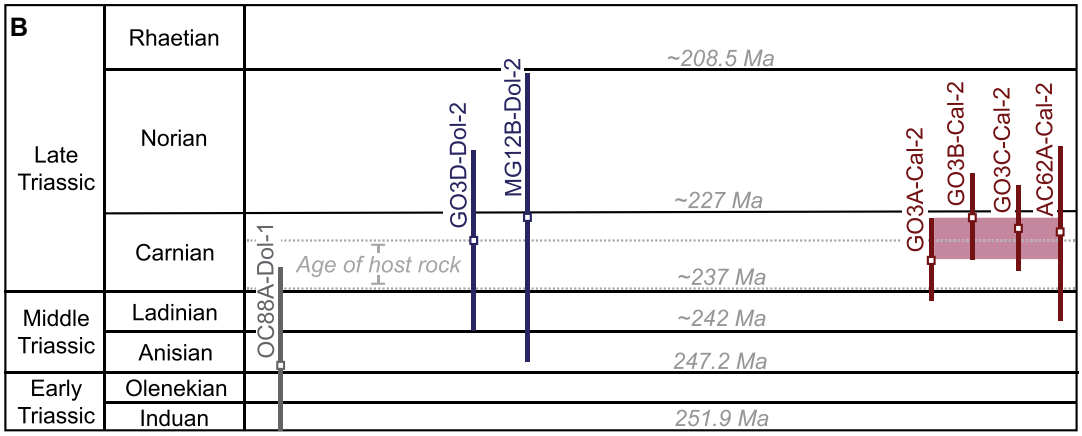

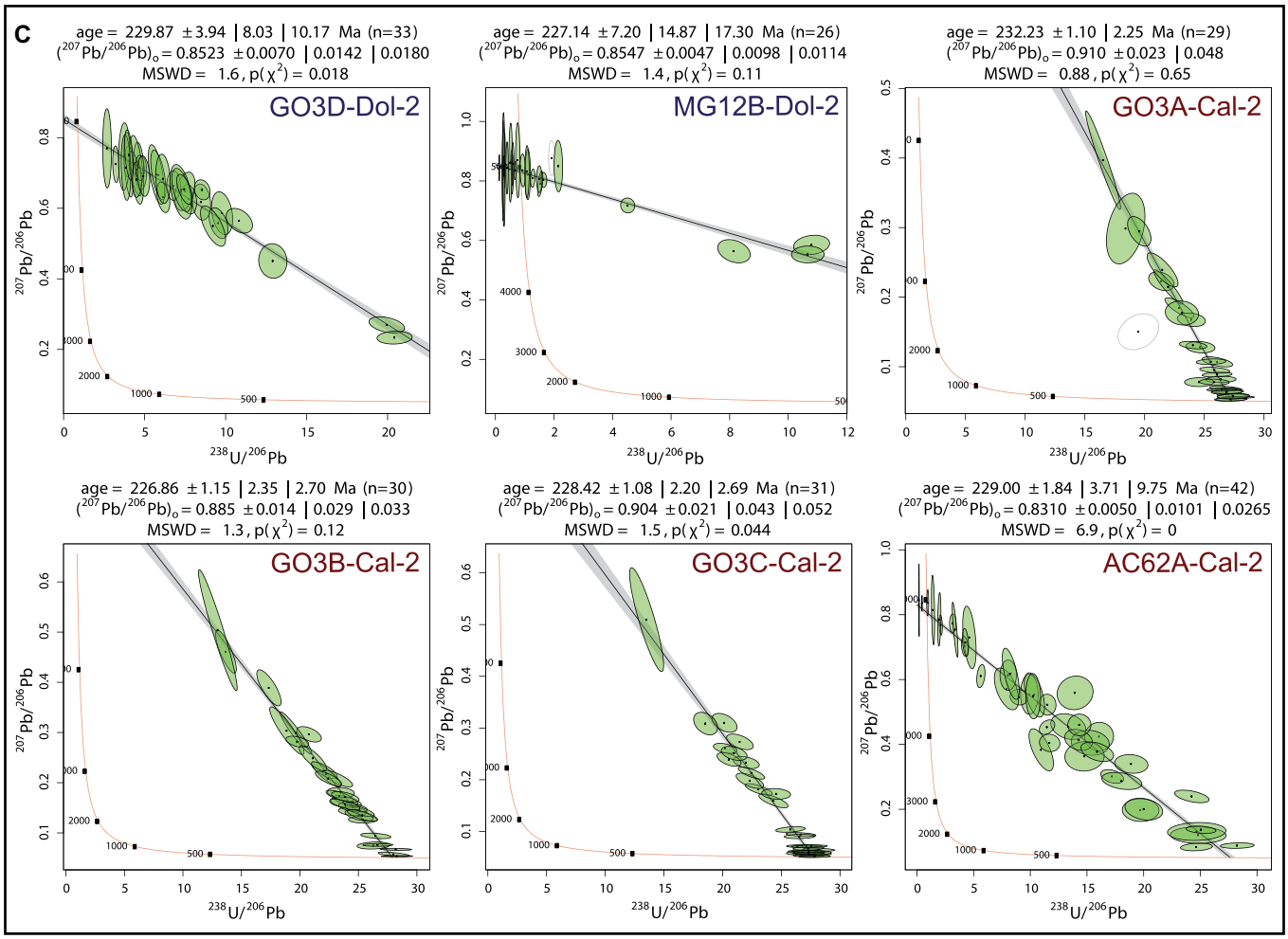

age data, any correlation between precipitation temperatures and burial depths is highly questionable, and inferences about geodynamic settings remain speculative. The term MVT encompasses a broad range of sulfide deposits formed under different conditions and should thus be used with a purely descriptive meaning, avoiding genetic implications.

ACKNOWLEDGMENTS

We thank Altamin, Ltd. (Perth, Australia), for the fruitful collaboration. T. Blaise, D. Chew, an anonymous reviewer, and editor W. Clyde provided constructive suggestions. This paper is dedicated to the memory of P. Rossetti, who first conceptualized the idea of this research.

REFERENCES CITED

Altamin, Ltd., 2021, ASX announcement—Major mineral resource upgrade at Gorno: https://clients3.weblink.com.au/pdf/AZI/02395048.pdf (accessed August 2021).

Assereto, R., Jadoul, F., and Omenetto, P., 1977, Stratigrafia e metallogenesi del settore occidentale del distretto a Pb, Zn, fluorite e barite di Gorno (Alpi Bergamasche): Rivista Italiana di Paleontologia e Stratigrafia, v. 83, p. 395–532.

Berra, F., and Carminati, E., 2010, Subsidence history from a backstripping analysis of the Permo-Mesozoic succession of the central southern Alps (northern Italy): Basin Research, v. 22, p. 952–975, https://doi.org/10.1111/j.1365-2117.2009.00453.x.

Brannon, J.C., Cole, S.C., Podosek, F.A., Ragan, V.M., Coveney, R.M., Wallace, M.W., and Bradley, A.J., 1996, Th-Pb and U-Pb dating of ore-stage calcite and Paleozoic fluid flow: Science, v. 271, p. 491–493, https://doi.org/10.1126/science.271.5248.491.

Brigo, L., Kostelka, L., Omenetto, P., Schneider, H.-J., Schroll, E., Schulz, O., and Štrucl, I., 1977, Comparative reflections on four Alpine Pb-Zn deposits, *in* Klemm, D.D., and Schneider, H.-J., eds., Time and Strata-Bound Ore Deposits: Berlin, Springer, p. 273–293, https://doi.org/10.1007/978-3-642-66806-7_18.

Cerny, I., 1989, Die karbonatgebundenen Blei-Zink-Lagerstätten des alpinen und ausser-alpinen Mesozoikums: Die Bedeutung ihrer Geologie, Stratigraphie und Faziesgebundenheit für Prospektion und Bewertung: Archiv für Lagerstättenforschung der Geologischen Bundesanstalt, v. 11, p. 5–125.

De Min, A., Velicogna, M., Ziberna, L., Chiaradia, M., Alberti, A., and Marzoli, A., 2020, Triassic magmatism in the European southern Alps as an early phase of Pangea break-up: Geological Magazine, v. 157, p. 1800–1822, https://doi.org/10.1017/S0016756820000084.

Doglioni, C., 1987, Tectonics of the Dolomites (southern Alps, northern Italy): Journal of Structural Geology, v. 9, p. 181–193, https://doi.org/10.1016/0191-8141(87)90024-1.

Grandia, F., Asmerom, Y., Getty, S., Cardellach, E., and Canals, À., 2000, U-Pb dating of MVT ore-stage calcite: Implications for fluid flow in a Mesozoic extensional basin from Iberian Peninsula: Journal of Geochemical Exploration, v. 69–70, p. 377–380, https://doi.org/10.1016/S0375-6742(00)00030-3.

Guillong, M., Wotzlaw, J.F., Looser, N., and Laurent, O., 2020, Evaluating the reliability of U-Pb laser ablation inductively coupled plasma mass spectrometry (LA-ICP-MS) carbonate geochronology: Matrix issues and a potential calcite validation reference material: Geochronology, v. 2, p. 155–167, https://doi.org/10.5194/gchron-2-155-2020.

Henjes-Kunst, E., Raith, J.G., and Boyce, A.J., 2017, Micro-scale sulfur isotope and chemical variations in sphalerite from the Bleiberg Pb-Zn deposit, eastern Alps, Austria: Ore Geology Reviews, v. 90, p. 52–62, https://doi.org/10.1016/j.oregeorev.2017.10.020.

Hnatyshin, D., Creaser, R.A., Wilkinson, J.J., and Gleeson, S.A., 2015, Re-Os dating of pyrite confirms an early diagenetic onset and extended duration of mineralization in the Irish Zn-Pb ore field: Geology, v. 43, p. 143–146, https://doi.org/10.1130/G36296.1.

Hou, Y., Azmy, K., Berra, F., Jadoul, F., Blamey, N.J.F., Gleeson, S.A., and Brand, U., 2016, Origin of the Breno and Esino dolomites in the western southern Alps (Italy): Implications for a volcanic influence: Marine and Petroleum Geology, v. 69, p. 38–52, https://doi.org/10.1016/j.marpetgeo.2015.10.010.

Jadoul, F., Berra, F., Bini, A., Ferliga, C., Mazzoccola, D., Papani, L., Piccin, A., Rossi, R., Rossi, S., and Trombetta, G.L., 2012, Note Illustrative della Carta Geologica d'Italia alla Scala 1:50.000, Foglio 077 "Clusone": Treviso, Italy, Servizio Geologico d'Italia, ISPRA (Istituto Superiore per la Protezione e la Ricerca Ambientale), Regione Lombardia, 120 p.

Jaupart, C., and Mareschal, J.-C., 2007, Heat flow and thermal structure of the lithosphere, *in* Schubert, G., and Watts, A.B., eds., Crustal and Lithosphere Dynamics: Treatise on Geophysics, Volume 6, p. 217–251, https://doi.org/10.1016/B978-044452748-6.00104-8.

Jicha, H.L., 1951, Alpine lead-zinc ores of Europe: Economic Geology, v. 46, p. 707–730, https://doi.org/10.2113/gsecongeo.46.7.707.

Kesler, S.E., Chesley, J.T., Christensen, J.N., Hagni, R.D., Heijlen, W., Kyle, J.R., Muchez, P., Misra, K.C., and Van der Voo, R., 2004, Discussion of "Tectonic controls of Mississippi Valley–type lead-zinc mineralization in orogenic forelands" by D.C. Bradley and D.L. Leach: Mineralium Deposita, v. 39, p. 512–514, https://doi.org/10.1007/s00126-004-0422-3.

Kucha, H., Schroll, E., Raith, J.G., and Halas, S., 2010, Microbial sphalerite formation in carbonate-hosted Zn-Pb ores, Bleiberg, Austria: Micro to nanotextural and sulfur isotope evidence: Economic Geology, v. 105, p. 1005–1023, https://doi.org/10.2113/econgeo.105.5.1005.

Laubscher, H.P., 1985, Large-scale, thin-skinned thrusting in the southern Alps: Kinematic models: Geological Society of America Bulletin, v. 96, p. 710–718, https://doi.org/10.1130/0016-7606(1985)96<710:LTTITS>2.0.CO;2.

Leach, D.L., Bradley, D., Lewchuk, M.T., Symons, D.T.A., de Marsily, G., and Brannon, J., 2001, Mississippi Valley–type lead-zinc deposits through geological time: Implications from recent age-dating research: Mineralium Deposita, v. 36, p. 711–740, https://doi.org/10.1007/s001260100208.

Leach, D.L., Bechstädt, T., Boni, M., and Zeeh, S., 2003, Triassic-hosted Mississippi Valley–type zinc-lead ores of Poland, Austria, Slovenia, and Italy, *in* Kelly, J.G., et al., eds., Europe's Major Base Metal Deposits: Dublin, Irish Association of Economic Geologists, p. 169–213.

Leach, D.L., Sangster, D.F., Kelley, K.D., Large, R.R., Garven, G., Allen, C.R., Gutzmer, J., and Walters, S., 2005, Sediment-hosted lead-zinc deposits: A global perspective: Economic Geology, v. 100, p. 561–607, https://doi.org/10.5382/AV100.18.

Maucher, A., and Schneider, H.-J., 1967, The Alpine lead-zinc ores, *in* Brown, J.S., ed., Genesis of Lead-Zinc-Barite-Fluorite Deposits in Carbonate Rocks (Mississippi Valley Type Deposits): Economic Geology Monograph 3, p. 71–89, https://doi.org/10.5382/Mono.03.

Mondillo, N., Lupone, F., Boni, M., Joachimski, M., Balassone, G., De Angelis, M., Zanin, S., and Granitzio, F., 2019, From Alpine-type sulfides to nonsulfides in the Gorno Zn project (Bergamo, Italy): Mineralium Deposita, v. 55, p. 953–970, https://doi.org/10.1007/s00126-019-00912-5.

Omenetto, P., 1966, Il giacimento piombo-zincifero di Oltre il Colle (Alpi bergamasche): Memorie degli Istituti di Geologia e Mineralogia dell'Università di Padova, v. 25, p. 3–49.

Ostendorf, J., Henjes-Kunst, F., Mondillo, N., Boni, M., Schneider, J., and Gutzmer, J., 2015, Formation of Mississippi Valley–type deposits linked to hydrocarbon generation in extensional tectonic settings: Evidence from the Jabali Zn-Pb-(Ag) deposit (Yemen): Geology, v. 43, p. 1055–1058, https://doi.org/10.1130/G37112.1.

Ostendorf, J., Henjes-Kunst, F., Schneider, J., Melcher, F., and Gutzmer, J., 2017, Genesis of the carbonate-hosted Tres Marias Zn-Pb-(Ge) deposit, Mexico: Constraints from Rb-Sr sphalerite geochronology and Pb isotopes: Economic Geology, v. 112, p. 1075–1087, https://doi.org/10.5382/econgeo.2017.4502.

Roberts, N.M.W., Rasbury, E.T., Parrish, R.R., Smith, C.J., Horstwood, M.S.A., and Condon, D.J., 2017, A calcite reference material for LA-ICP-MS U-Pb geochronology: Geochemistry Geophysics Geosystems, v. 18, p. 2807–2814, https://doi.org/10.1002/2016GC006784.

Schroll, E., Köppel, V., and Cerny, I., 2006, Pb and Sr isotope and geochemical data from the Pb-Zn deposit Bleiberg (Austria): Constraints on the age of mineralization: Mineralogy and Petrology, v. 86, p. 129–156, https://doi.org/10.1007/s00710-005-0107-3.

Shelton, K.L., Hendry, J.P., Gregg, J.M., Truesdale, J.P., and Somerville, I.D., 2019, Fluid circulation and fault- and fracture-related diagenesis in Mississippian syn-rift carbonate rocks on the northeast margin of the metalliferous Dublin Basin, Ireland: Journal of Sedimentary Research, v. 89, p. 508–536, https://doi.org/10.2110/jsr.2019.31.

Zanchetta, S., Malusà, M.G., and Zanchi, A., 2015, Precollisional development and Cenozoic evolution of the Southalpine retrobelt (European Alps): Lithosphere, v. 7, p. 662–681, https://doi.org/10.1130/L466.1.

Zanchi, A., D'Adda, P., Zanchetta, S., and Berra, F., 2012, Syn-thrust deformation across a transverse zone: The Grem–Vedra fault system (central southern Alps, N Italy): Swiss Journal of Geosciences, v. 105, p. 19–38, https://doi.org/10.1007/s00015-011-0089-6.

Printed in USA